Supplementary Information

Synthesis of N_2-Type Supreatomic Molecule

Ryohei Saito,[†‡] Katsuhiro Isozaki,[†‡]* Yoshiyuki Mizuhata,[†]and Masaharu Nakamura[†‡]*

[†]International Research Center for Elements Science, Institute for Chemical Research, Kyoto University, Gokasyo, Uji, Kyoto 611-0011, Japan.

[‡]Department of Energy and Hydrocarbon Chemistry, Graduate School of Engineering, Kyoto University, Nishikyoku, Kyoto 615-8510, Japan.

E-mail: kisozaki@scl.kyoto-u.ac.jp, masaharu@scl.kyoto-u.ac.jp

Contents

Experimental Section

Instruments. Proton nuclear magnetic resonance (^{1}H NMR) and phosphorous nuclear magnetic resonance (^{31}P NMR) spectra were recorded on JEOL ECS-400NR (392 MHz) and ECZL-400R (399 MHz) spectrometers. Proton chemical shift values are reported in parts per million (ppm, δ scale) downfield from tetramethylsilane and are referenced to the tetramethylsilane (δ 0.00). ^{31}P NMR chemical shift values are reported in parts per million (ppm, δ scale) downfield from H_3PO_4 and are referenced to the H_3PO_4 (δ 0.00) as the external standard. Data are presented as: chemical shift, multiplicity (s = singlet, d = doublet, t = triplet, q = quartet, quint = quintet, sext = sextet, sept = septet, m = multiplet and/or multiplet resonances, br = broad), coupling constant in hertz (Hz), signal area integration in natural numbers, and assignment (*italic*). The high precision isotope peak intensities ratios were determined by Fourier transformation-ion cyclotron resonance-mass spectrometry (FT-ICR-MS) coupled with electron spray ionization (ESI) technique using a solariX FT-ICR-MS spectrometer (Bruker Daltonics GmbH). UV−Vis absorption spectra were recorded on a Shimadzu UV-2700 spectrometer. Photochemical reactions were carried out using Asahi Spectra MAX-303 Xe light sources. The photo-irradiation power was measured by HIOKI optical power meter 3664. Single crystal X-ray diffraction date were collected on a Bruker-D8 Venture diffractometer. Graphite monochromated Mo *K*α radiation was used as the X-ray source. Data reductions were performed using Bruker SAINT software. Structures were solved by direct methods (SHELXT)[1] and refined against F^2 by weighted full matrix least-squares (SHELXL).[2]

Materials. Materials were purchased from Wako, Tokyo Chemical Industry Co., Ltd., Nakalai tesque, Inc., and other commercial suppliers, and were used without further purification, unless otherwise noted. Ethanol (EtOH), acetonitrile (MeCN), palladium(II) acetate ($Pd(OAc)_2$), ammonium hexanitratocerate(IV) ($(NH_4)_2[Ce(NO_3)_6]$), cesium acetate (CsOAc), and sodium borohydride ($NaBH_4$) were purchased from Wako. 12 M Hydrochloric acid was purchased from Nacalai tesque. Tetrachloroauric(III) acid tetrahydrate ($HAuCl_4{\cdot}4H_2O$) was purchased from TANAKA KIKINNZOKU KOGYO K. K. Diethylphenylphosphine (depp) was purchased from Sigma-Aldrich. 2,2'-Thiodiethanol and Dichloro(1,5-cyclooctadiene)platinum(II) ($PtCl_2$(cod)) were purchased from TCI. Chloroform ($CHCl_3$), dichloromethane (CH_2Cl_2), methanol (MeOH), hexane, toluene, and ethyl acetate (EtOAc) were purchased from Kishida Chemical Co., Ltd. Chloroform-*d* was purchased from Cambridge Isotope Laboratories, Inc. Au(depp)Cl was

[1] Sheldrick, G. M. *Acta Cryst. A* **2015,** *71,* 3–8.

[2] Sheldrick, G. M. *Acta Cryst. C* **2015,** *71,* 3–8.

synthesized according to the literature method.[3]

General procedure for the photo-induced synthesis of $Pd_2Au_{17}(depp)_{10}Cl_7$ 2a

$PdAu_{12}(depp)_8Cl_4$ (**1a**, 10.0 mg, 2.5 mmol) was dissolved in the written solvent (8 mL) and Ar gas was bubbled into the solution 30 min in the dark. Then, visible light (385–740 nm) was irradiated to the solution. After the photo-irradiation for 5 h, the solvent was removed using a rotary evaporator and the residue was purified by preparative thin-layer chromatography (PTLC) eluted with hexane:AcOEt = 3:4. Crystallization was carried out by a vapor-diffusion of hexane to a toluene solution to afford black-red crystal of the titled compound.

Synthesis of $Pd_2Au_{17}(depp)_{10}Cl_7$ 2a by CAN-oxidation

$PdAu_{12}(depp)_8Cl_4$ (**1a**, 10.0 mg, 2.5 mmol) was dissolved in a mixture solvent of DCM and MeOH in a 1:3 ratio (8 mL) and Ar gas was bubbled into the solution for 30 minutes in the dark. Then, fleshly prepared CAN (ammonium hexanitratocerate (IV)) (1.4 mg, 2.5 mmol) solution in MeOH (100 μL) was added to the solution and stirred for 5 h in the dark. Then, the solvent was removed by rotary evaporator and purified in the above-mentioned procedure.

Synthesis of $Pt_2Au_{17}(depp)_{10}Cl_7$ 2b by photo-irradiation

$PtAu_{12}(depp)_8Cl_4$ (**1b**, 10.0 mg, 2.5 mmol) was dissolved in a mixture solvent of DCM and MeOH in a 1:3 ratio (8 mL) and Ar gas was bubbled into the solution for 30 minutes in the dark. Then, visible light (385–740 nm) was irradiated to the solution. After the photo-irradiation for 1 h, the solvent was removed using a rotary evaporator and the residue was purified by preparative thin-layer chromatography (PTLC) eluted with hexane:AcOEt = 3:4. Crystallization was carried out by a vapor-diffusion of hexane to DCM/EtOH (1:1) solution to afford black-yellow crystal of the titled compound.

---

[3] Hooper, T. N.; Butts, C. P.; Green, M.; Haddow, Mairi. F.; McGrady, J. E.; Russell, C. A. *Chem. Eur. J.* **2009**, *15*, 12196–12200.

Synthesis of $PdAu_{12}(depp)_8Cl_4$ 1a

A solution was prepared by stirring (depp)AuCl (0.28 g, 0.72 mmol) and $Pd(OAc)_2$ (15.2 mg, 68 μmol) in a mixture of DCM and MeOH in a 1:1 ratio (30 mL) for 5 min. Upon adding freshly prepared 6.0 mL solution of $NaBH_4$ (30.2 mg, 0.80 mmol) in ethanol to this mixture, the solution quickly turned brown. The reaction was allowed to proceed for 4 h at rt, after which the solvent was removed using a rotary evaporator. The resulting residue was then dissolved in EtOH, and 5.6 μL of 12 M hydrochloric acid (HCl) was added to the solution. The mixture was stirred for an additional 3 h in the dark, then dried again using the rotary evaporator. The residue was purified by column chromatography eluted with $CHCl_3$:MeOH = 5:95. Crystallization was carried out by a vapor-diffusion of hexane to a toluene solution to afford black crystal of the titled compound (70. 0 mg, 26%).

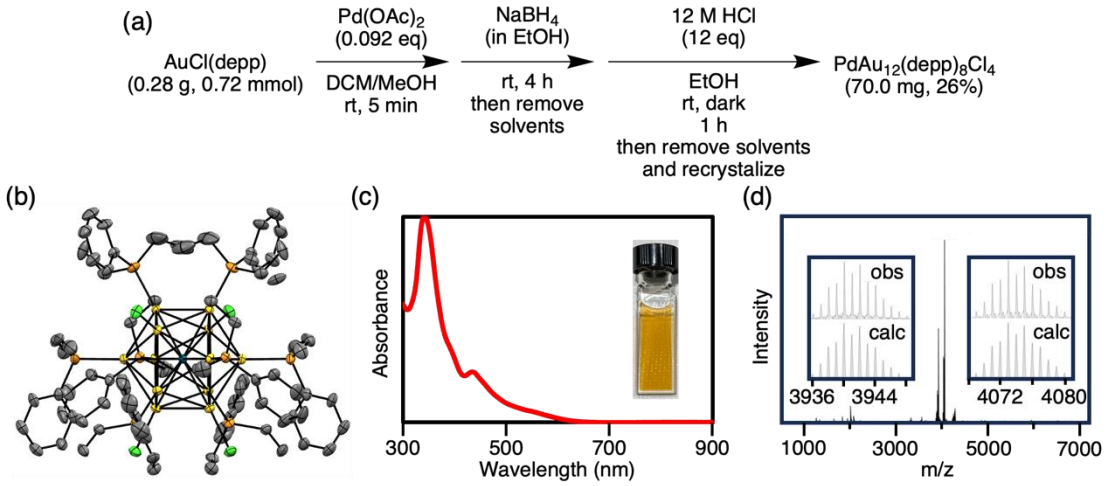

Figure S1. (a) Synthetic scheme of $PdAu_{12}(depp)_8Cl_4$ **1a**. (b) ORTEP drawing of **1a** with thermal ellipsoids in 50% probability level. H and disordered atoms are omitted for clarify. (c) UV–vis absorption spectrum in DCM. (d) ESI-Mass spectrum of **1a** in DCM. The inset shows the observed and calculated isotope patterns: $[M]^+$ and $[M+Cs]^+$.

Synthesis of $PtAu_{12}(depp)_8Cl_4$ 1b

A solution of (depp)AuCl (71.8 mg, 0.18 mmol) and $PtCl_2(cod)$ (6.2 mg, 17 μmol) was prepared by stirring in a mixture solvent of DCM and MeOH (1:1 ratio, 15 mL) for 5 minutes. Upon adding freshly prepared 1.5 mL solution of $NaBH_4$ (7.6 mg, 0.20 mmol) in ethanol to this mixture, the solution quickly turned brown. The reaction was allowed to proceed for 4 h at rt, after which the solvent was removed using a rotary evaporator. The residue was purified by column chromatography eluted with $CHCl_3$:MeOH = 95:5. Crystallization was carried out by a vapor-diffusion of hexane to a toluene solution to afford orange crystal of the titled compound (15.1 mg, 22%).

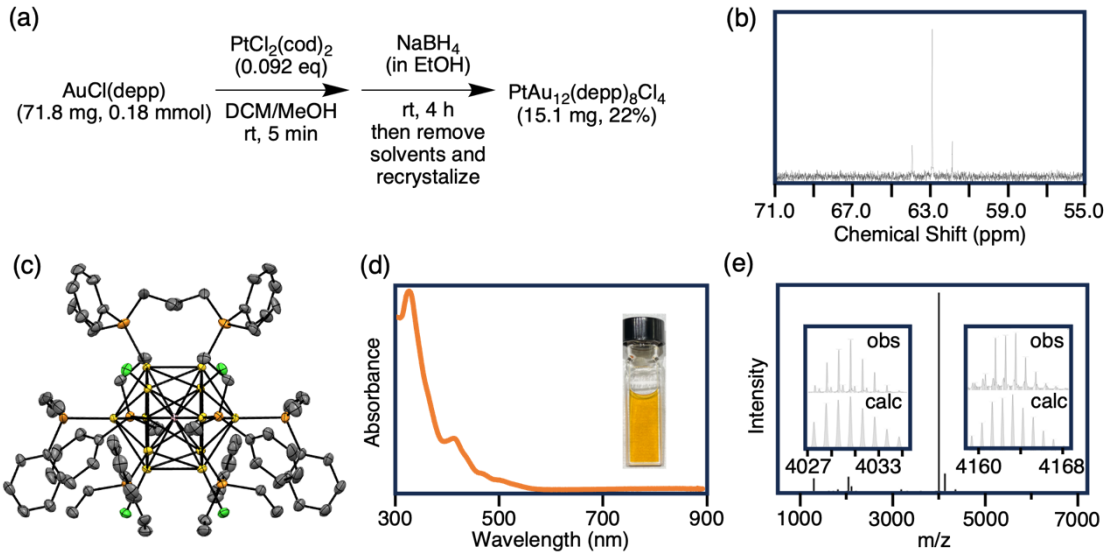

Figure S2. (a) Synthetic scheme of $PtAu_{12}(depp)_8Cl_4$ **1b**. (b)^{31}PNMR spectrum for a $CDCl_3$ solution of **1b**. (c) ORTEP drawing of **1b** with thermal ellipsoids in 50% probability level. H and disordered atoms are omitted for clarify. (d) UV–vis absorption spectrum in DCM. (e) ESI-Mass spectrum of **1b** in DCM. The inset shows the observed and calculated isotope patterns: $[M]^+$ and $[M+Cs]^+$.

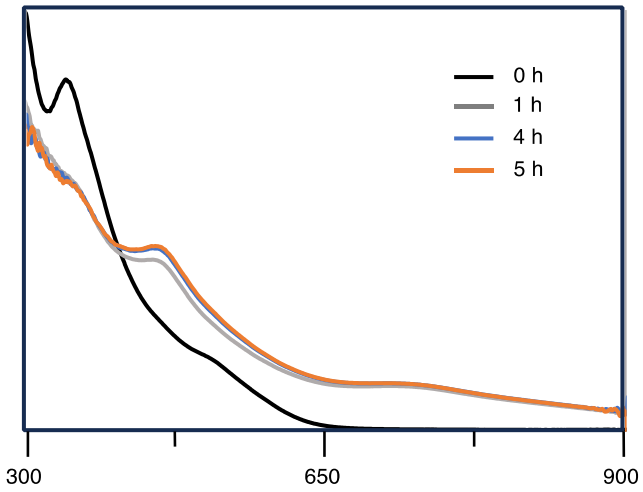

Figure S3. Time-course absorption spectra of **1a** in MeOH/CH_2Cl_2 solution under the irradiation of visible light (385–740 nm).

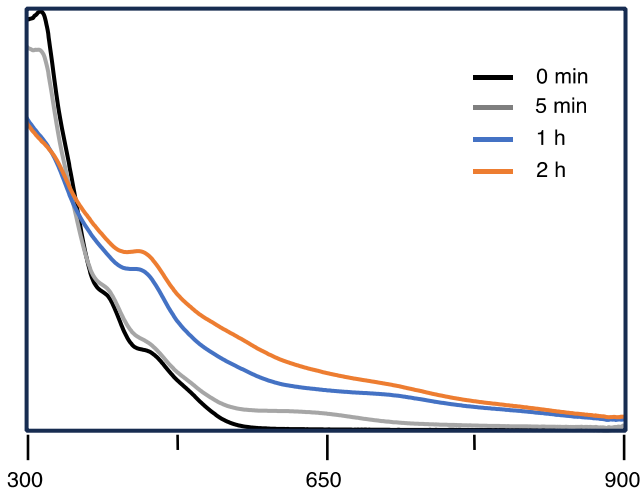

Figure S4. Time-course absorption spectra of (a) **1b** in MeOH/CH_2Cl_2 solution under the irradiation of visible light (385–740 nm).

Theoretical calculation

Geometry optimization of nanoclusters were studied through DFT calculations using the B3LYP functional with Grimme's D3BJ dispersion correction.[4] Basis sets used were LanL2dz for Au, Pd, Pt and 6-31G(d) for Cl, P, C, and H atoms. Singlet spin states were assumed for ground states geometries of nanoclusters. Structural optimization was carried out followed by frequency calculations to confirm that the optimized structures had no imaginary frequencies, indicating that they were located at the local/global minima of the potential energy surfaces. All other calculations were conducted using the Gaussian 16 program.[5]

[4] Grimme, S.; Ehrlich, S.; Goerigk, L. Effect of the Damping Function in Dispersion Corrected Density Functional Theory, *J. Comput. Chem.* **2011,** *32*, 1456–1465.

[5] Gaussian 16, Revision C.01, Frisch, M. J.; Trucks, G. W.; Schlegel, H. B.; Scuseria, G. E.; Robb, M. A.; Cheeseman, J. R.; Scalmani, G.; Barone, V.; Petersson, G. A.; Nakatsuji, H.; Li, X.; Caricato, M.; Marenich, A. V.; Bloino, J.; Janesko, B. G.; Gomperts, R.; Mennucci, B.; Hratchian, H. P.; Ortiz, J. V.; Izmaylov, A. F.; Sonnenberg, J. L.; Williams-Young, D.; Ding, F.; Lipparini, F.; Egidi, F.; Goings, J.; Peng, B.; Petrone, A.; Henderson, T.; Ranasinghe, D.; Zakrzewski, V. G.; Gao, J.; Rega, N.; Zheng, G.; Liang, W.; Hada, M.; Ehara, M.; Toyota, K.; Fukuda, R.; Hasegawa, J.; Ishida, M.; Nakajima, T.; Honda, Y.; Kitao, O.; Nakai, H.; Vreven, T.; Throssell, K.; Montgomery, J. A., Jr.; Peralta, J. E.; Ogliaro, F.; Bearpark, M. J.; Heyd, J. J.; Brothers, E. N.; Kudin, K. N.; Staroverov, V. N.; Keith, T. A.; Kobayashi, R.; Normand, J.; Raghavachari, K.; Rendell, A. P.; Burant, J. C.; Iyengar, S. S.; Tomasi, J.; Cossi, M.; Millam, J. M.; Klene, M.; Adamo, C.; Cammi, R.; Ochterski, J. W.; Martin, R. L.; Morokuma, K.; Farkas, O.; Foresman, J. B.; Fox, D. J. Gaussian, Inc., Wallingford CT, 2016.

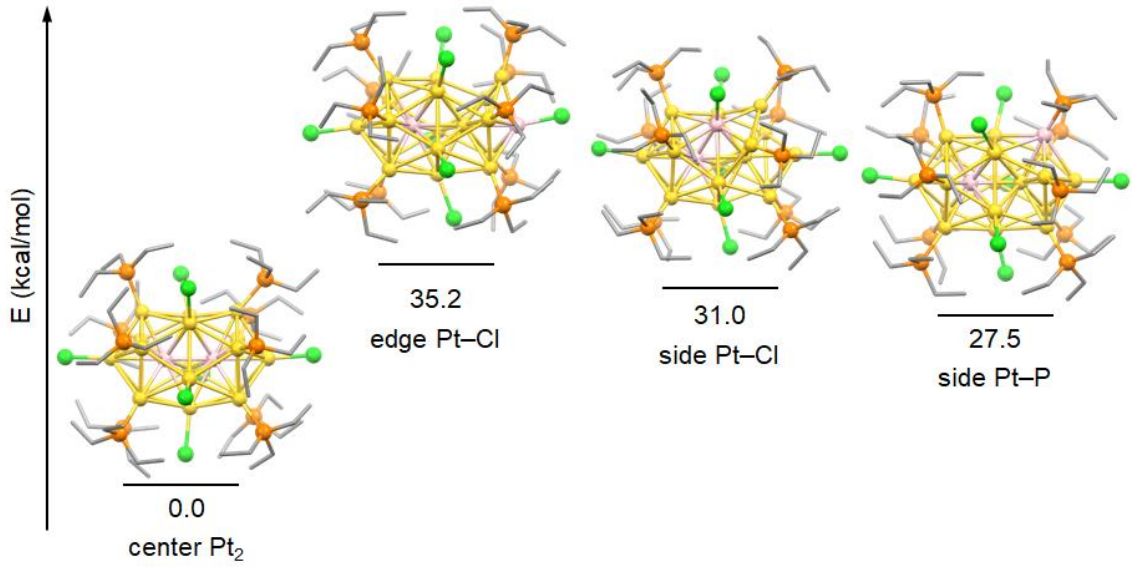

Figure S5. DFT-calculated energy diagram of regioisomers of $Pt_2Au_{17}(PEt_3)_{10}Cl_7$ with different Pt positions.

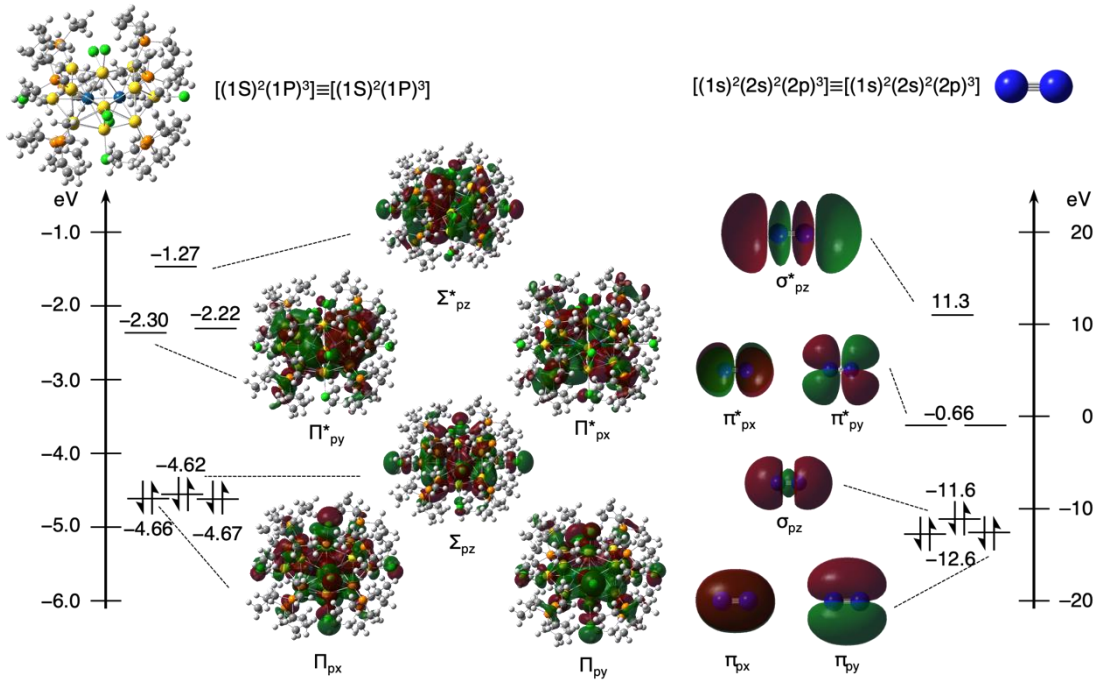

Figure S6. Energy diagrams and schematic Kohn–Sham orbitals of $Pt_2Au_{17}(PEt_3)_{10}Cl_7$ (left) and N_2 molecule (right).

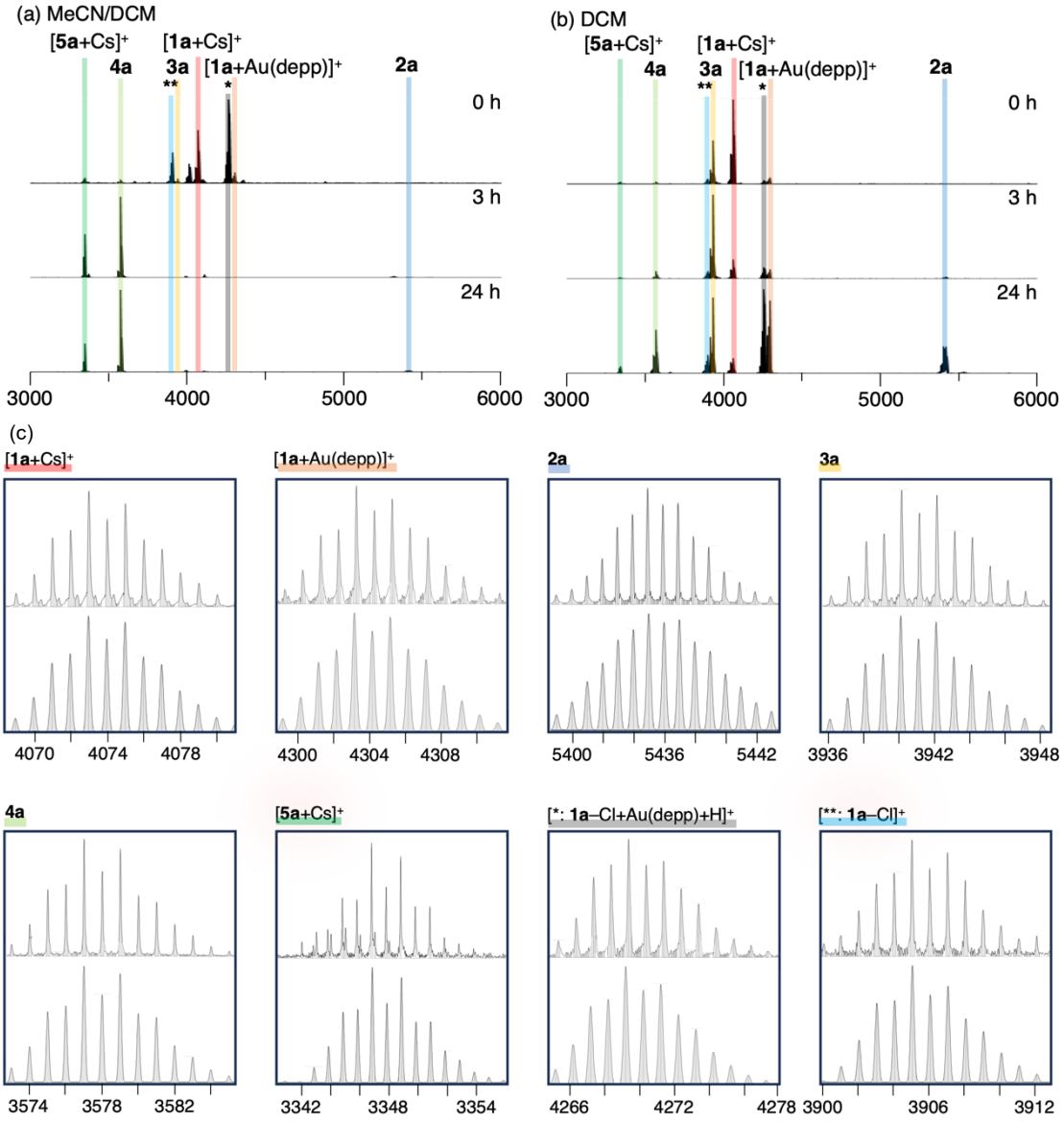

Figure S7. Time-course ESI-Mass spectra from **1a** to **2a** under the light irradiation: (a) MeCN/DCM and (b) DCM solution. (c) shows the detected fragments (top) and theoretical isotopic patterns (bottom).

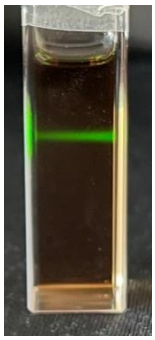

Figure S8. Photograph of green laser-irradiated solution of **1a** after the photo-induced reaction. The Tyndal effect was observed, suggesting the formation of nanoparticles in the solution during the photo-induced reaction.

Scheme S1. Plausible reaction mechanism from **1a** to **2a**.

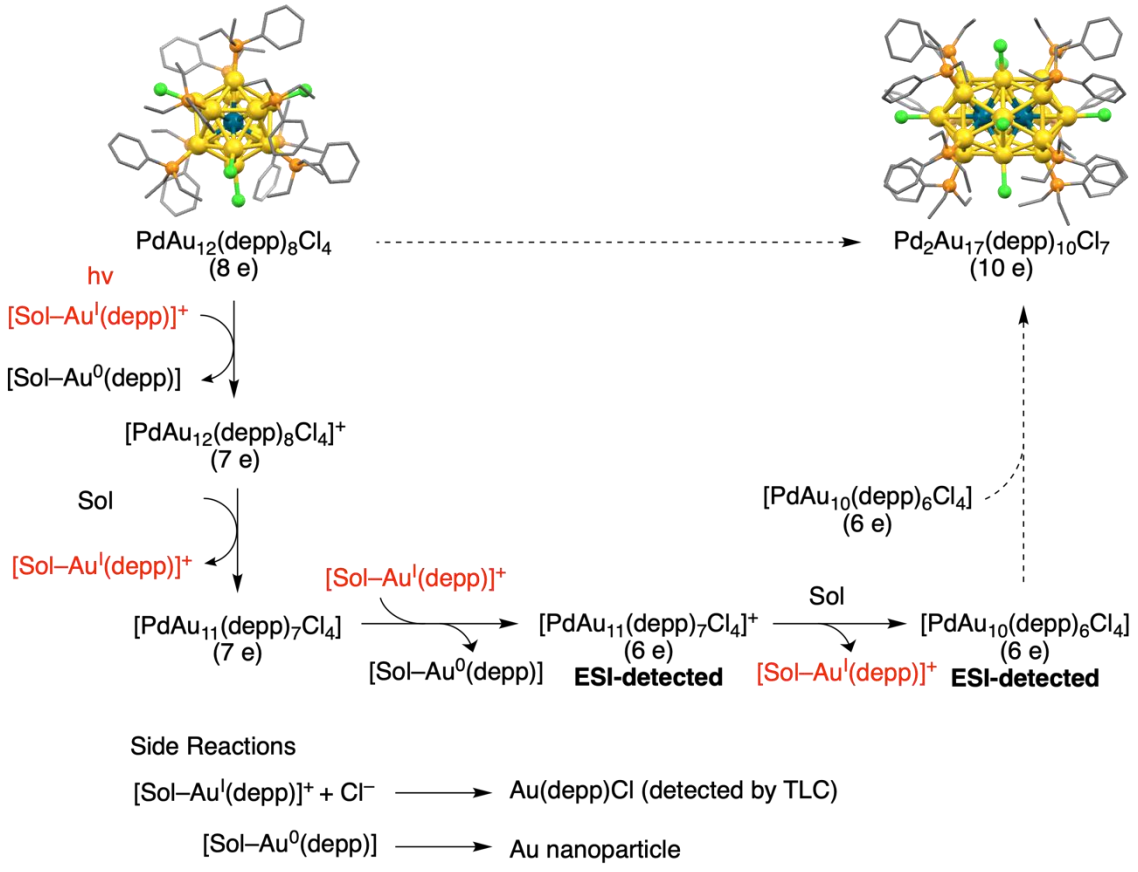

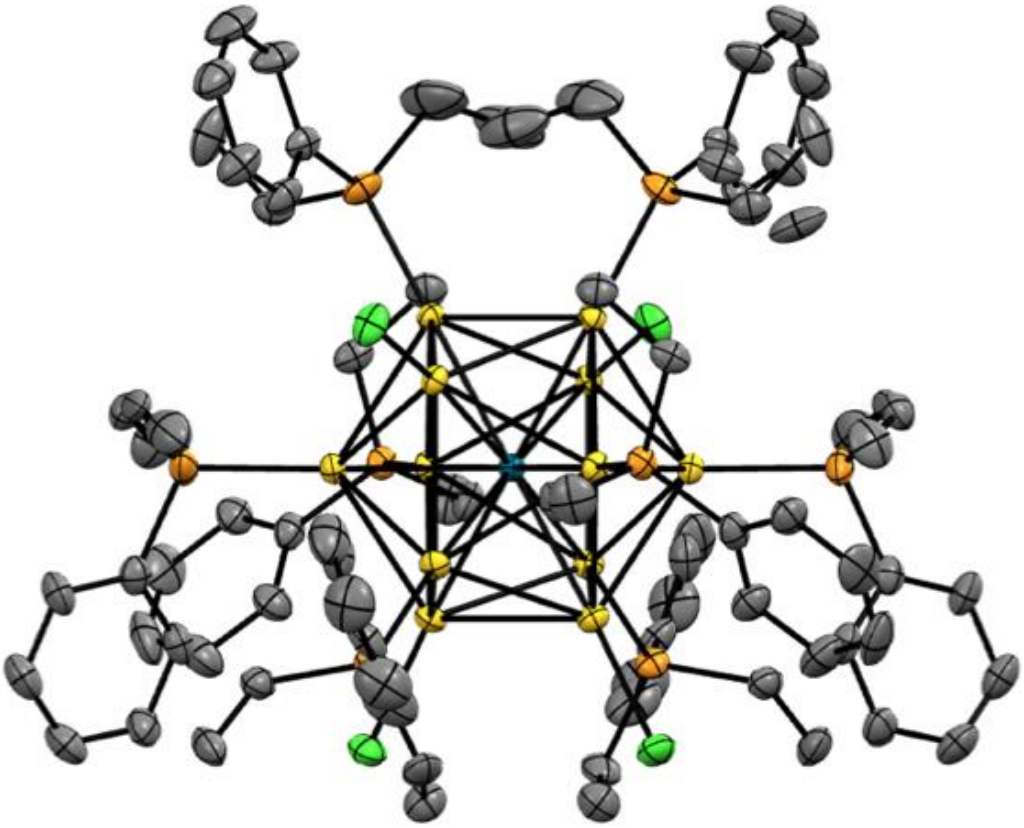

Figure S9. ORTEP drawing of **1a** with thermal ellipsoids in 50% probability level. H and disordered atoms are omitted for clarify.

Table S1. Crystallographic Data for 1a

Formula	$C_{80}H_{120}Au_{12}Cl_4P_8Pd$
FW (g mol^{-1})	3941.31
Crystal size (mm)	0.06 × 0.05 × 0.04
Crystal system	Monoclinic
Space group	*C* 2/c
Z	4
a (Å)	28.281(2)
b (Å)	13.8952(10)
c (Å)	25.5604(17)
α (°)	90
β (°)	113.183(2)
γ (°)	90
Cell Volume (Å^3)	9233.4
Temperature (K)	90(3)
ρ_{calc} (g cm^{-3})	2.835
μ (mm^{-1})	19.466
θ range (°)	2.61–27.49
Measured reflections	121535
Unique reflections	10604 (R_{int}=0.0983)
Data/restrains/parameters	10604/0/515
R indices [$I > 2\sigma(I)$]	R_1 = 0.0296, $_wR_2$ = 0.0602
R indices [all data]	R_1 = 0.0378, $_wR_2$ = 0.0632
Goodness-of-fit on F^2	1.027

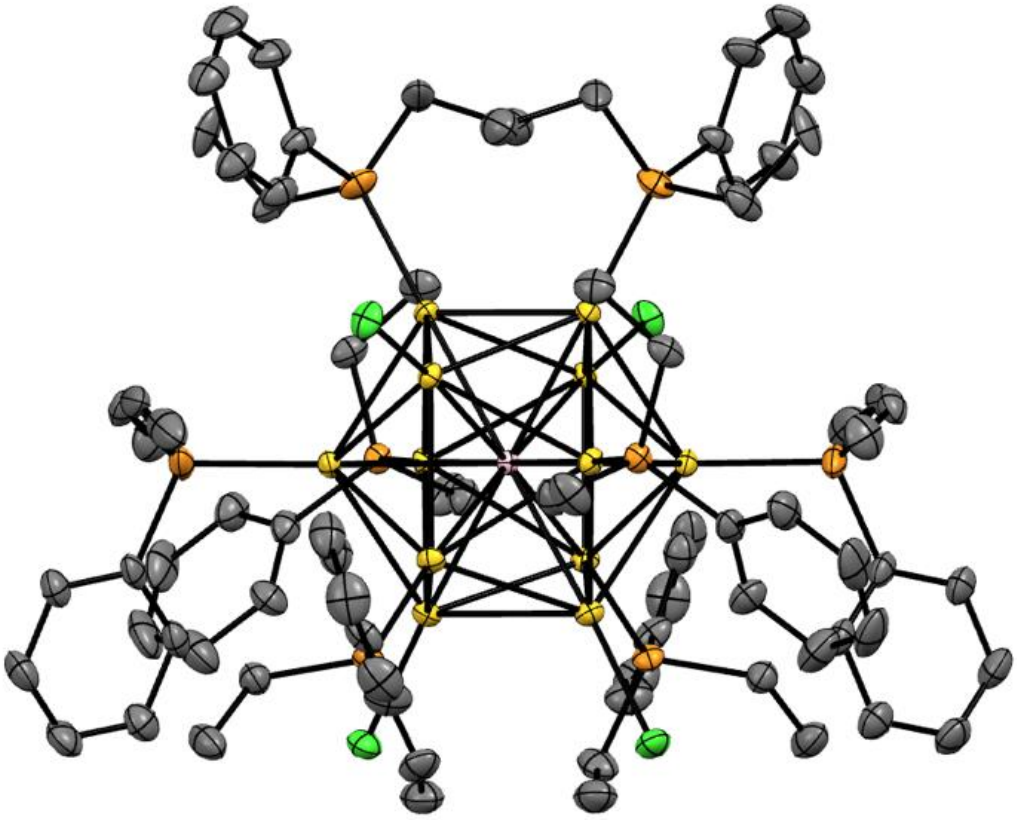

Figure S10. ORTEP drawing of **1b** with thermal ellipsoids in 50% probability level. H and disordered atoms are omitted for clarify.

Table S2. Crystallographic Data for 1b

Formula	$C_{80}H_{120}Au_{12}Cl_4P_8Pt$
FW (g mol^{-1})	4030.00
Crystal size (mm)	0.04 × 0.11 × 0.11
Crystal system	Monoclinic
Space group	*C* 2/c
Z	4
a (Å)	28.2646(9)
b (Å)	13.8659(5)
c (Å)	25.5195(8)
α (°)	90
β (°)	113.1540(10)
γ (°)	90
Cell Volume (Å^3)	9233.4
Temperature (K)	90(3)
ρ_{calc} (g cm^{-3})	2.911
μ (mm^{-1})	20.870
θ range (°)	2.615–30.051
Measured reflections	145860
Unique reflections	13473 (R_{int}=0.0473)
Data/restrains/parameters	13473/0/517
R indices [$I > 2\sigma(I)$]	R_1 = 0.0241, $_wR_2$ = 0.0557
R indices [all data]	R_1 = 0.0315, $_wR_2$ = 0.0597
Goodness-of-fit on F^2	1.027

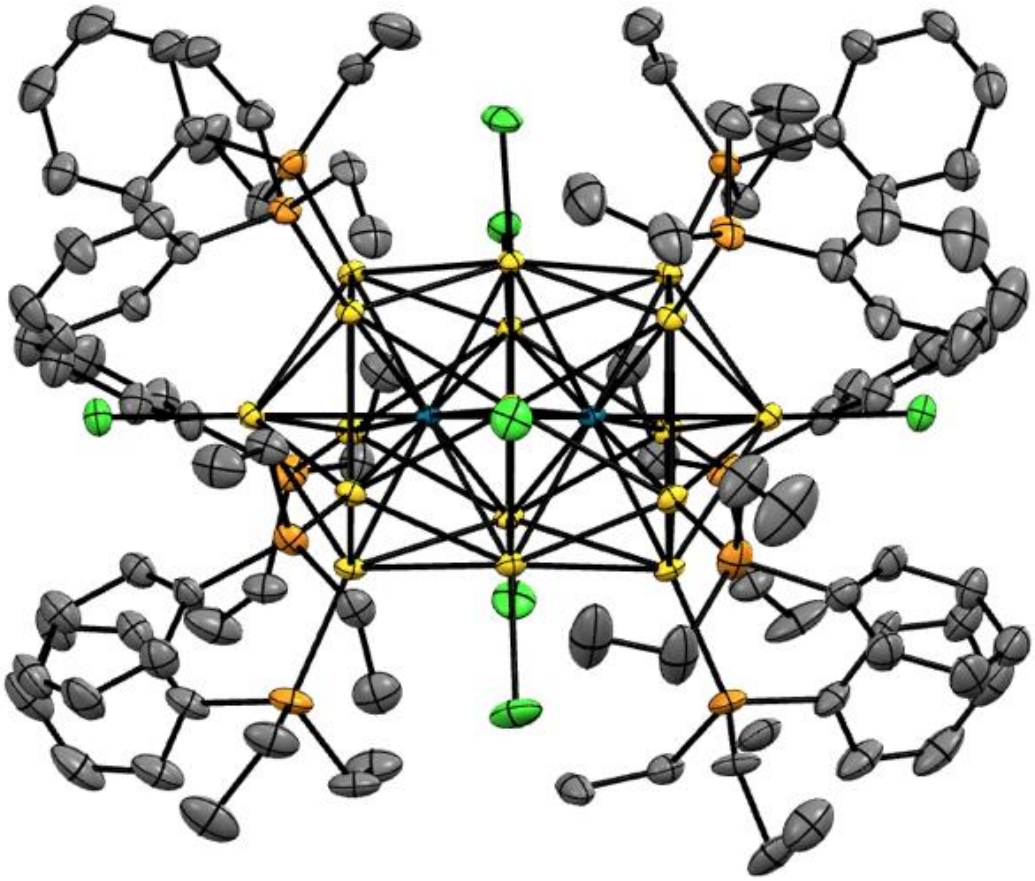

Figure S11. ORTEP drawing of **2a** with thermal ellipsoids in 50% probability level. H and disordered atoms are omitted for clarify.

Table S3. Crystallographic Data for 2a

Formula	$C_{100}H_{150}Au_{17}Cl_7P_{10}Pd_2$
FW (g mol^{-1})	5471.27
Crystal size (mm)	0.07 × 0.07 × 0.1
Crystal system	Monoclinic
Space group	$P\,2_1/c$
Z	4
a (Å)	18.5668(9)
b (Å)	33.8678(15)
c (Å)	23.1062(11)
α (°)	90
β (°)	92.002(2)
γ (°)	90
Cell Volume (Å^3)	14520.7(12)
Temperature (K)	90(2)
ρ_{calc} (g cm^{-3})	2.503
μ (mm^{-1})	17.611
θ range (°)	1.863–27.476
Measured reflections	580158
Unique reflections	33165 (R_{int}=0.0628)
Data/restrains/parameters	33165/0/1371
R indices [$I > 2\sigma(I)$]	R_1 = 0.0265, $_wR_2$ = 0.0622
R indices [all data]	R_1 = 0.0402, $_wR_2$ = 0.0685
Goodness-of-fit on F^2	1.148

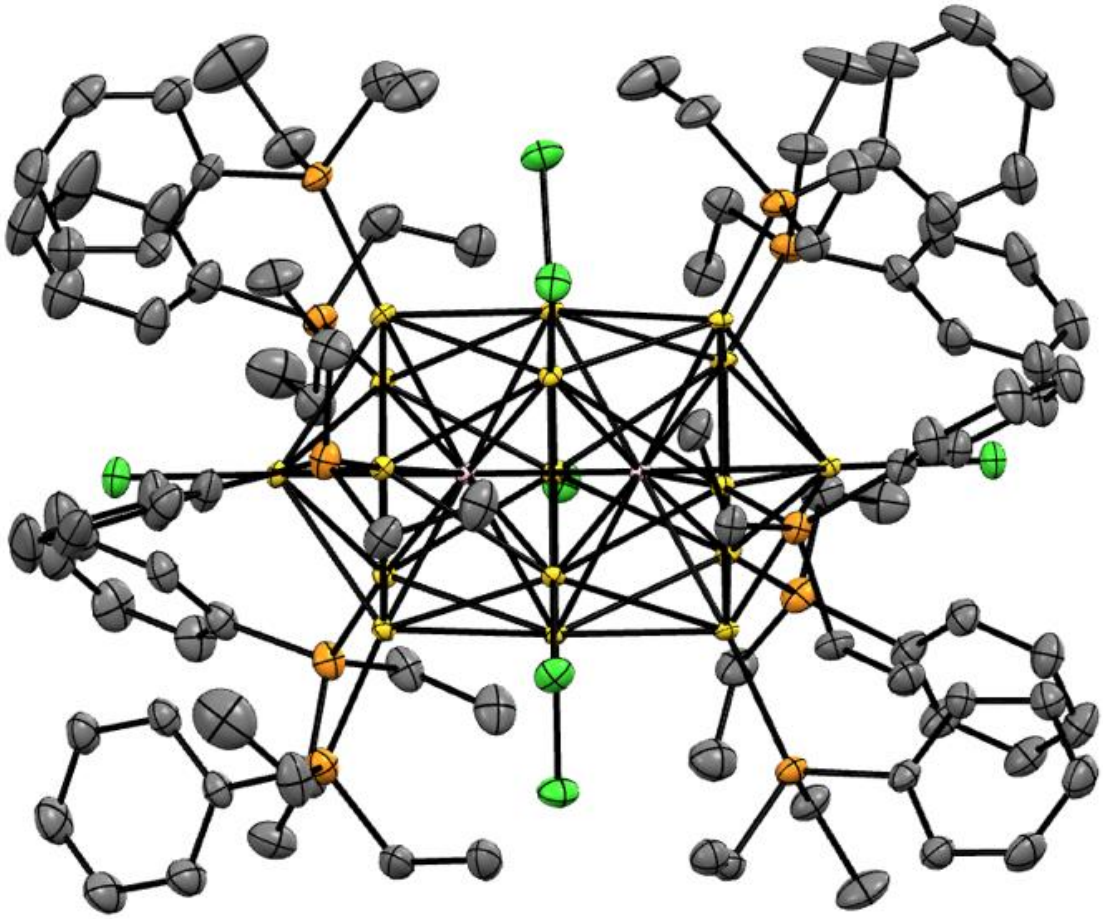

Figure S12. ORTEP drawing of **2b** with thermal ellipsoids in 50% probability level. H and disordered atoms are omitted for clarify.

Table S4. Crystallographic Data for 2b

Formula	$C_{100}H_{150}Au_{17}Cl_7P_{10}Pt_2$
FW (g mol^{-1})	5648.65
Crystal size (mm)	0.04 × 0.1 × 0.16
Crystal system	Triclinic
Space group	$P\bar{1}$
Z	4
a (Å)	17.1273(6)
b (Å)	18.6246(6)
c (Å)	20.3473(6)
α (°)	97.4360(10)
β (°)	93.8170(10)
γ (°)	93.0860(10)
Cell Volume (Å^3)	6410.3(4)
Temperature (K)	90(2)
ρ_{calc} (g cm^{-3})	2.927
μ (mm^{-1})	21.846
θ range (°)	1.834–30.092
Measured reflections	769922
Unique reflections	37486 (R_{int}=0.0627)
Data/restrains/parameters	37486/0/1371
R indices [$I > 2\sigma(I)$]	R_1 = 0.0265, $_wR_2$ = 0.0622
R indices [all data]	R_1 = 0.0402, $_wR_2$ = 0.0685
Goodness-of-fit on F^2	1.148

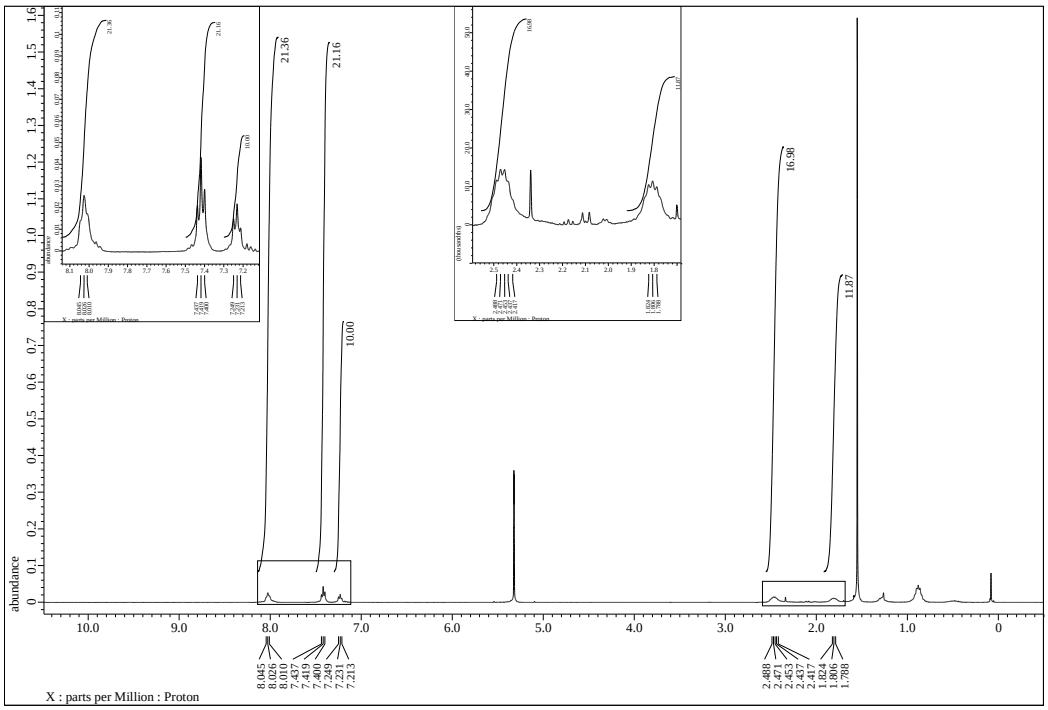

Figure S13. ^{1}H NMR spectrum (392 MHz, DCM-d_2) of **2a**.

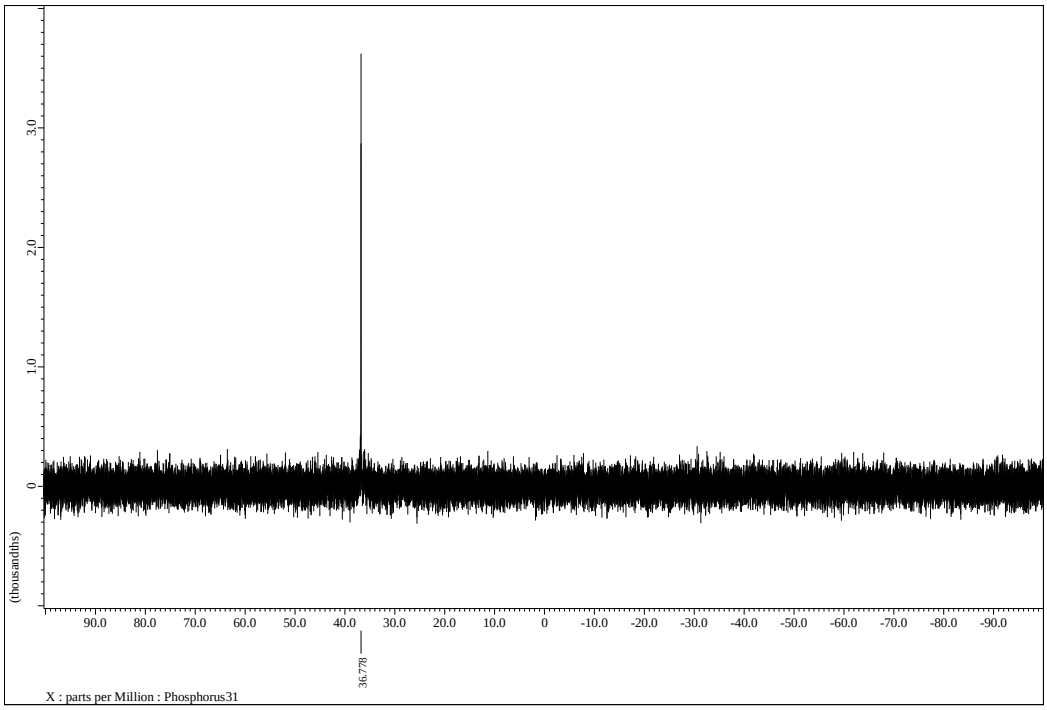

Figure S14. ^{31}P NMR spectrum (162 MHz, DCM-d_2) of **2a**.

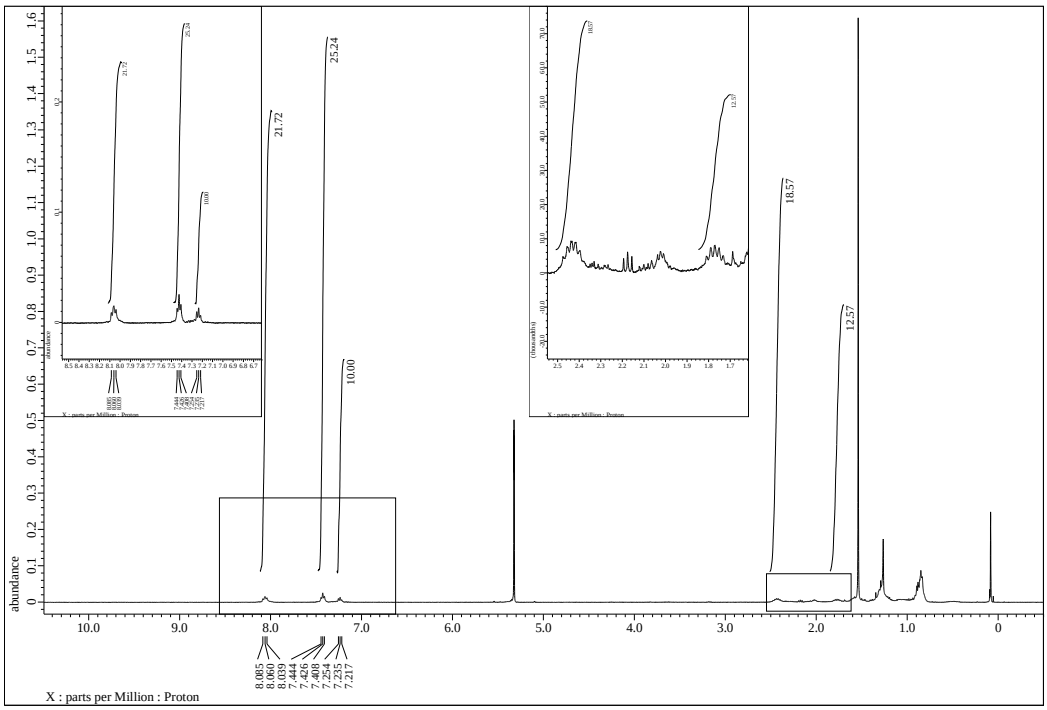

Figure S15. ^{1}H NMR spectrum (392 MHz, DCM-d_2) of **2b**.

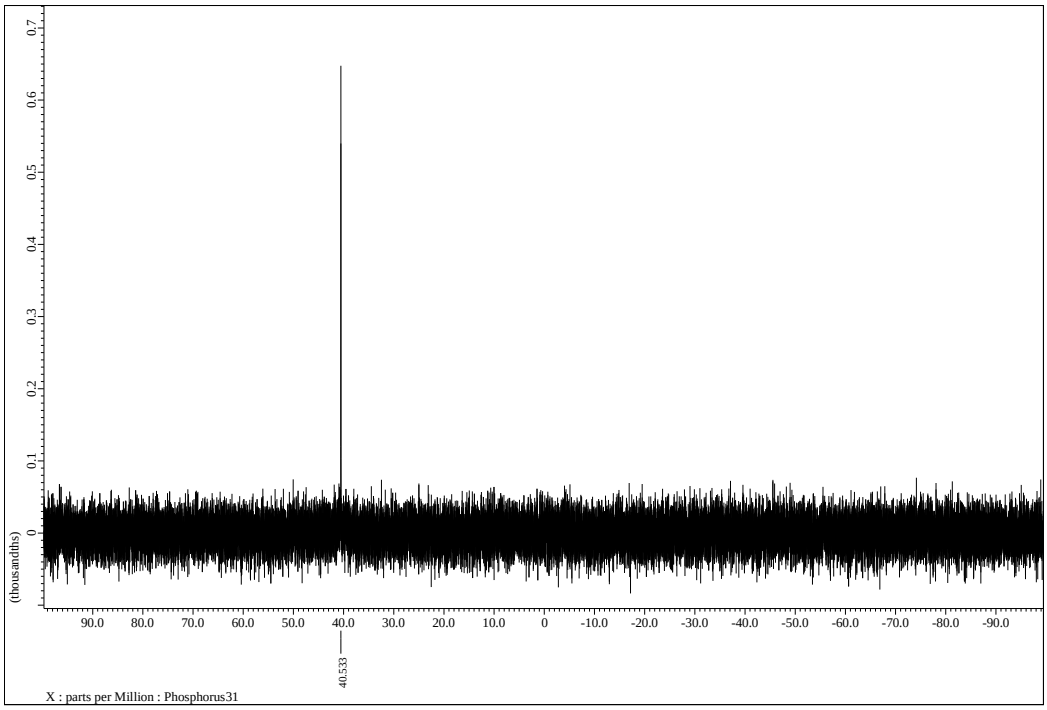

Figure S16. ^{31}P NMR spectrum (162 MHz, DCM-d_2) of **2b**.